

# Fast slip with inhibited temperature rise due to mineral dehydration: Evidence from experiments on gypsum

Nicolas Brantut<sup>1</sup>, Raehee Han<sup>2,3</sup>, Toshihiko Shimamoto<sup>2</sup>, Nathaniel Findling<sup>1</sup>, and Alexandre Schubnel<sup>1</sup>

<sup>1</sup>Laboratoire de Géologie, CNRS UMR 8538, École Normale Supérieure, 75005 Paris, France

<sup>2</sup>Department of Earth and Planetary Systems Science, Hiroshima University, Higashi-Hiroshima 739-8526, Japan

<sup>3</sup>Geologic Environment Division, Korea Institute of Geoscience and Mineral Resources, Daejeon 305-350, South Korea

## ABSTRACT

Anomalously low heat flow around active faults has been a recurrent subject of debate over past decades. We present a series of high-velocity friction experiments on gypsum rock cylinders showing that the temperature of the simulated fault plane is efficiently buffered due to large-scale endothermic dehydration reaction. The tests were performed at 1 MPa normal stress and a velocity of 1.3 m s<sup>-1</sup>, while measuring the temperature close to the sliding surface and the relative humidity around the sample. The temperature close to the sliding surface is remarkably stable at ~100 °C during the dehydration reaction of gypsum. Microstructural and X-ray diffraction investigations show that dehydration occurs at the very beginning of the test, and progresses into the bulk as slip increases. In the hottest parts of the sample, anhydrite crystal growth is observed. The half-thickness of the dehydrated layer ranges from 160 μm at 2 m slip to 5 mm at 68 m slip. Thermodynamic estimates of the energy needed for the dehydration to occur yield values ranging from 10% to 50% of the total mechanical work input. The temperature plateau is thus well explained by the energy sink due to the dehydration reaction and the phase change from liquid water into steam. We suggest that similar endothermic reactions can efficiently buffer the temperature of fault zones during an earthquake. This is a way to explain the low heat flow around active faults and the apparent scarcity of frictional melts in nature.

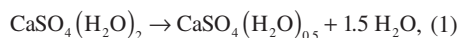
## INTRODUCTION

A recurrent issue in fault zone studies is the low or absent temperature and heat flux anomalies along seismically active faults (Lachenbruch and Sass, 1980). The temperature of a fault zone is closely related to the shear stress acting on it during its motion. Applying a simple Coulomb friction law with a constant friction coefficient of 0.6 or 0.8 within a slipping zone a few centimeters or millimeters thick induces an elevated shear stress that should trigger rapid and ubiquitous melting of the fault rocks during a seismic event. However, geological records of seismically induced frictional melt are relatively scarce (e.g., Sibson, 2003; Sibson and Toy, 2006). Among other hypotheses, it has been suggested that faults may be statically strong but dynamically weak. Several dynamic fault-weakening mechanisms have been recognized from experimental and theoretical works: silica gel formation of SiO<sub>2</sub>-rich rocks (Goldsby and Tullis, 2002; Di Toro et al., 2004), thermal pressurization of pore fluids (Sibson, 1973; Lachenbruch, 1980; Mase and Smith, 1985, 1987; Andrews, 2002; Rice, 2006), and flash heating (Rice, 1999, 2006).

In addition, recent studies of rapid phase changes during high-velocity friction (HVF) tests (Hirose and Bystricky, 2007; Han et al., 2007, 2010; Brantut et al., 2008) have emphasized the possible importance of chemical reactions at the time scale of an earthquake. Thermal decomposition reactions are generally endothermic

processes. Theoretical studies (Sulem and Famin, 2009; Brantut et al., 2010) have reported that the temperature on the fault plane can be kept relatively low due to the latent heat of reaction, if the reactions are fast enough to occur during a fast slip event.

To test such a hypothesis, we performed HVF tests on solid gypsum blocks. Gypsum is a hydrous calcium sulfate [or CaSO<sub>4</sub>(H<sub>2</sub>O)<sub>2</sub>] that dehydrates at ~100 °C to form bassanite [CaSO<sub>4</sub>(H<sub>2</sub>O)<sub>0.5</sub>], and bassanite turns into anhydrite at slightly higher temperature (~140 °C):



During the tests, shear stress, temperature, and relative humidity were continuously recorded. Microstructural and X-ray diffraction (XRD) analysis were performed on the tested samples, and a gross energy budget is analyzed to infer the amount of mechanical energy converted into latent heat of reaction. We discuss the possible consequences of such processes in nature during a large earthquake.

## MATERIALS AND METHODS

Experiments were performed in a rotary HVF apparatus at Hiroshima University (Shimamoto and Hirose, 2006; Togo et al., 2009; see also Fig. DR1 in the GSA Data Repository<sup>1</sup>). The normal stress applied on the simulated fault was

$\sigma \sim 1$  MPa, and the slip rate was held constant at 1.3 m s<sup>-1</sup>. The tested material was initially pure gypsum polycrystals from Volterra (Italy). The specimen geometry is a pair of solid cylinders with an outer diameter  $R$  of 24.95 mm (Fig. 1A). Due to the rotary geometry of the samples, all the results are interpreted in terms of equivalent slip and slip rate. Assuming that shear stress  $\tau$  is homogeneous on the sliding surface of area  $S = \pi R^2$ , an equivalent velocity  $V_{\text{eq}}$  can be written as:

$$\tau V_{\text{eq}} S = \iint_S \tau \omega r \, dS, \quad (3)$$

where  $\omega$  is the angular velocity (in rad s<sup>-1</sup>), which implies (Hirose and Shimamoto, 2005)

$$V_{\text{eq}} = \frac{2}{3} \omega R. \quad (4)$$

Thus, the equivalent slip, hereafter referred to as “displacement,” (respectively slip rate) corresponds to the slip (respectively slip rate) at two-thirds of the total radius. Mechanical data are reported in terms of effective friction, calculated as the ratio  $\tau/\sigma$ .

All tests were performed at room temperature and room humidity. The atmosphere around the sample was not confined. The temperature inside the gypsum blocks was measured by two K-type thermocouples (TC), located 0.9 mm (TC1) and 4.5 mm (TC2), respectively, from the sliding surface (Fig. 1B; see also Fig. DR2). The precise vertical position of the TC tip cannot be known, so we only report an approximate position ( $\pm 0.2$  mm). High-temperature ceramic bond was used to fix the TC positions. Relative humidity around the sample was measured with a capacitance type sensor placed ~2 cm from the sample surface. Prior to each test, we applied a few bars of axial load and grinded slowly, at a few tens of rotations per minute, the sample end surfaces one on each other. This ensured a good matching of the sliding surfaces and prevented the sample edges from breaking during

<sup>1</sup>GSA Data Repository item 2011035, specimen assembly, sketch of the HVF apparatus (Figure DR1), detailed sample set-up (Figure DR2), additional friction and temperature curves (Figure DR3), and complete XRD data (Figure DR4), is available online at [www.geosociety.org/pubs/ft2011.htm](http://www.geosociety.org/pubs/ft2011.htm), or on request from [editing@geosociety.org](mailto:editing@geosociety.org) or Documents Secretary, GSA, P.O. Box 9140, Boulder, CO 80301, USA.

fast motion. Prior to starting the test, the sliding surface was cleaned of the gouge produced.

## EXPERIMENTAL RESULTS

The typical frictional behavior of a pair of solid rock cylinders consists of a peak friction of 0.6 at the onset of slip, followed by a dramatic decrease down to 0.2 within the first 1 m

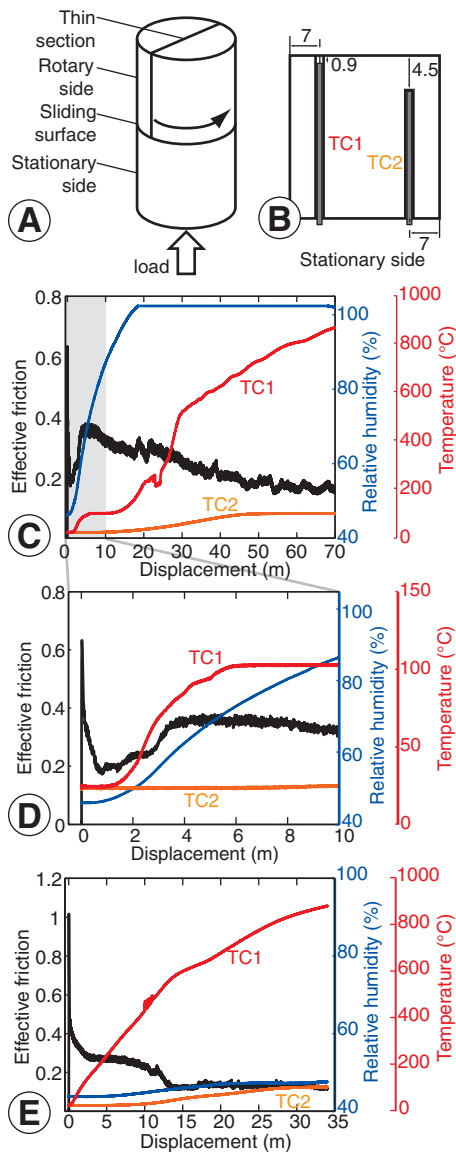


**Figure 1.** High-velocity friction (HVF) tests (positions in mm). **A:** Sample assembly. **B:** Positions of thermocouples. **C–E:** Effective friction in terms of friction coefficient (black), relative humidity (blue), and thermocouple outputs (red—TC1, orange—TC2) as functions of slip displacement during HVF tests performed at normal stress of 1 MPa and velocity of  $1.3 \text{ m s}^{-1}$ . **C:** Temperature close to sliding surface (TC1, red) is constant for  $\sim 10 \text{ m}$  at beginning of test. **D:** Close-up of first 10 m of slip. **E:** Second run on same sample after cooling at room temperature. No temperature plateau is recorded on TC1.

of displacement (Figs. 1C and 1D). Friction then increases to a second peak of 0.4 over 4 m of slip, and finally it decreases gradually over the next 30–40 m of slip down to 0.2. The onset of  $\text{H}_2\text{O}$  emission was detected at 0.5 m of slip, and the sensor is saturated after 16.5 m of slip. The temperature measured by TC1, i.e., at 0.9 mm from the sliding surface, starts increasing at 1.2 m of slip, and rises to  $100^\circ\text{C}$  at 5.8 m of slip. Then temperature remains constant for 6 m, and finally rises again to reach  $\sim 900^\circ\text{C}$  at the end of the test. The temperature at 4.5 mm from the sliding surface (TC2) starts increasing very slowly at 8 m, reaches  $100^\circ\text{C}$  at 50 m, and is kept constant at this value during the rest of the test. After this experiment was stopped, we let the sample come back to room temperature and room humidity without removing the applied load. Then, a second run was performed. The frictional behavior consists of a unique, initial peak friction of 1.0 and a subsequent weakening down to 0.25 over a slip weakening distance of 3 m; a second weakening is observed at 13 m of slip down to 0.15 in friction (Fig. 1E). The temperature recorded by TC1 increases continuously up to  $\sim 900^\circ\text{C}$  at 34 m of slip. The temperature measured with TC2 increases in a way similar to that of the first run, and remains constant at  $100^\circ\text{C}$  when it reaches this value. In similar tests performed on Carrara marble, Han et al. (2010) reported significantly higher temperature rise away from the slipping zone. Humidity starts to increase at 5 m of slip, and rises only from 43.8% to 47.3% at the end of the test.

We repeated the solid cylinders experiment 5 times and stopped the run at total displacements of 2, 8, 10, 35, and 68 m (see Fig. DR3). After each test one-half of the sample was kept for thin-sectioning and the surface of the other half was observed under scanning electron microscope (SEM). At 2 m of slip, the sliding surface consists of a very smooth slickenside made of grains of  $\sim 1 \mu\text{m}$  or less in diameter (Fig. 2A). In some parts of the surface, these small grains are aggregated to form desiccation figures, which is evidence of the presence of liquid water on the surface. Such features are not seen when slip displacement is larger, thus it is unlikely that it is due to post-experiment condensation of ambient humidity. In an additional test stopped at 60 m displacement, the sliding surface observed by SEM was formed of a compact assemblage of grains ranging from 5 to  $20 \mu\text{m}$  in diameter (Fig. 2B). Such a texture may be due to high-temperature recrystallization and grain growth close to the sliding surface; fine grains of  $1 \mu\text{m}$  in size are observed on the surface.

The samples were drilled step by step every  $500 \mu\text{m}$  and the powder was analyzed using XRD. A representative example is shown in Figure 3 (68 m slip; for other data, see Fig. DR4). Anhydrite is found in the first 4 mm, bassanite

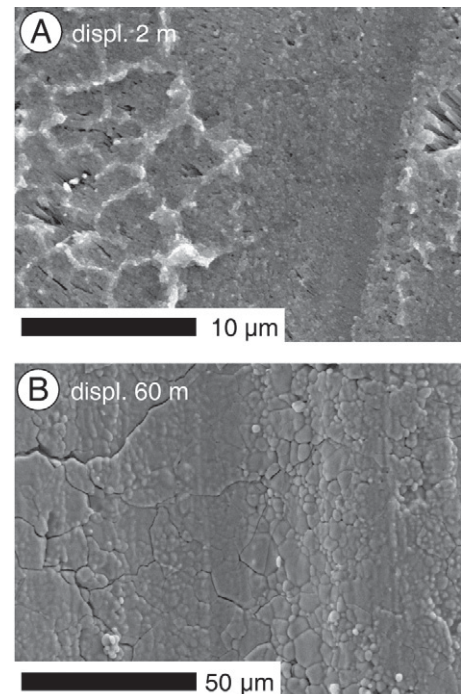


**Figure 2.** Representative scanning electron microscope photomicrographs of sliding surfaces of experimental samples. **A:** Sliding surface of sample after high-velocity friction (HVf) test conducted at 1 MPa normal stress,  $1.3 \text{ m s}^{-1}$ , and for 2 m slip (displ.—displacement). Grain size is  $\sim 1 \mu\text{m}$  or less. Desiccation marks are present on left. **B:** Sliding surface of sample after HVf test conducted at 1 MPa normal stress,  $1.3 \text{ m s}^{-1}$ , and for 60 m slip. Aggregates of small grains are found on very smooth and compact surface.

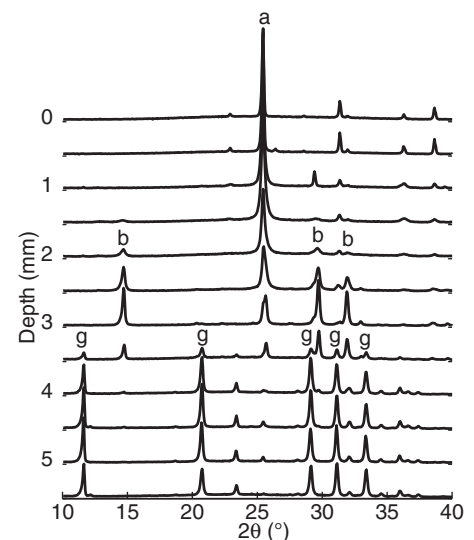


**Figure 3.** X-ray diffraction (XRD) spectra as function of depth for sample slid as much as 68 m. Sample was drilled and analyzed by steps of  $500 \mu\text{m}$ . Smooth transition from anhydrite (a) to bassanite (b) is observed below 2.5 mm, and transition to gypsum (g) is relatively sharp at 4.5 mm. Very low intensity anhydrite peaks are still found throughout sample, but they may be due to contamination by fine powder coming from upper surface of sample.

is found only between 2 and 4 mm, and gypsum appears clearly below 4 mm, where it is still mixed with a little anhydrite and bassanite. Below 5 mm, only gypsum is found. The thin sections display this evolution of the dehydrated zone with increasing displacement (Figs. 4A–4E). We calculate its mean thickness by measuring the dehydrated area on the thin section, divided by the diameter of the sample. It increases from 160  $\mu\text{m}$  at 2 m of slip, 610  $\mu\text{m}$  at 8 m, 1.120 mm at 10 m, 2.870 mm at 35 m, to 5.080 mm at 68 m of slip (Fig. 5). The transition from pure gypsum (transparent, rounded grains) to bassanite (brownish microliths) is relatively sharp, as seen in Figure 4F. It varies from a few tens of microns at 2 m slip to few hundreds of microns at elevated slip displacement. In the latter experiments, the anhydrite grains close to the

sliding surface have recrystallized (Fig. 4G) in the region of the sample that underwent the largest heat production.

#### INTERPRETATIONS AND DISCUSSION

Our observations show a large-scale dehydration reaction of gypsum during the HVF tests. The temperature plateau observed along the simulated fault zone can be explained considering that Reactions 1 and 2 are endothermic. The temperature plateau at the beginning of the tests is  $\sim 100^\circ\text{C}$ , which corresponds to the liquid-vapor transition of water. The reaction kinetic is thus fast enough to supply water continuously as friction occurs, which provides the heat sink buffering the temperature rise.

We estimate thermodynamically the energy needed to perform such reactions. The reaction

enthalpy is  $\Delta_f H^0 = 16.92 \text{ kJ mol}^{-1}$  from gypsum to anhydrite and liquid water, and  $\Delta_f H^0 = 98.17 \text{ kJ mol}^{-1}$  if water is released as vapor (Robie et al., 1979), neglecting the dependency of  $\Delta_f H$  with temperature. Starting from pure, nonporous gypsum the enthalpy per unit volume ranges from 453  $\text{MJ m}^{-3}$  to 2629  $\text{MJ m}^{-3}$ . Multiplying by the dehydrated thickness  $h$  we get an energy per unit surface  $E_c = h \times 453 \cdot 10^6 - h \times 2629 \cdot 10^6 \text{ J m}^{-2}$ . The total mechanical work  $W$  is calculated directly as the area below the friction curve. The relationship between  $E_c$  and  $W$  follows a linear trend (Fig. 5). The average ratio  $E_c/W$  ranges from 9% if we exclude water vaporization, to 52% when vaporization is complete. Considering that part of the dehydrated zone is actually bassanite and not anhydrite, and that only part of water is converted into steam, the real value may be between those extremes.

The low friction coefficient during the first weakening episode can be correlated to the inferred presence of liquid water on the surface. We have no evidence to distinguish whether the initial weakening is due to fluid pressure, hydrodynamic lubrication, or chemical effect. After dehydration of the sliding surface material, the lithology has changed, which may explain the second peak friction, along with the higher peak friction coefficient in the second run (Fig. 1D). The final slow weakening could be due to lubrication by aggregates or individual small grains disposed on the sliding surface, but no obvious interpretation can be drawn so far.

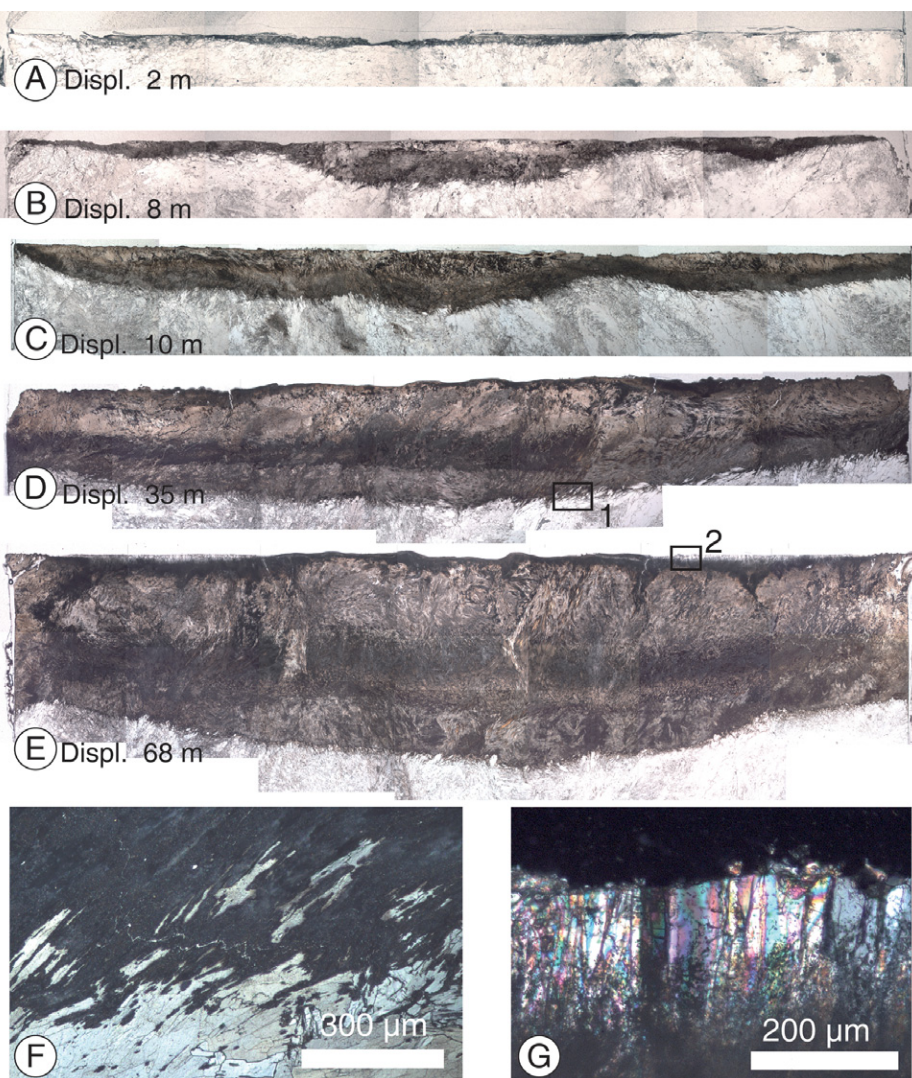


**Figure 4.** Photomicrographs of thin sections of samples deformed at 1 MPa normal stress,  $1.3 \text{ m s}^{-1}$ . A: Total displacement of 2 m. B: Total displacement of 8 m. C: Total displacement of 10 m. D: Total displacement of 35 m. E: Total displacement of 68 m. Total width of sample is 24.95 mm. Sliding surface is on top of each picture; rotation axis is at center. F: Close-up view of dehydration front located in area 1 (box in D). G: Recrystallization and grain growth of anhydrite close to sliding surface (area 2—box in E).

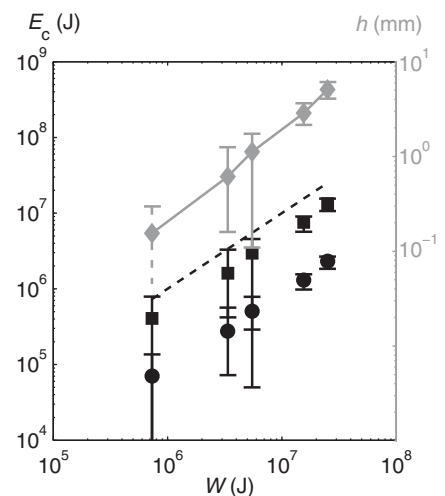


**Figure 5.** Energy ( $E_c$ ) needed to dehydrate gypsum thickness measured on thin sections (Figs. 3A–3E), as function of total mechanical work input ( $W$ ) during test. Circles correspond to dehydration of gypsum to anhydrite and liquid water; squares correspond to dehydration of gypsum to anhydrite and water vapor. Gray diamonds correspond to measured thickness  $h$ . Ratio between latent heat taken by reaction over mechanical work (dotted line of slope 1) ranges from 10% to 50%.

The case of gypsum could be viewed as an analogue of hydrous minerals (e.g., serpentines, clays, and phyllosilicates) that are commonly observed in major fault zones (Sulem et al., 2004; Solum et al., 2006; Hirono et al., 2008). Similarly to gypsum, they could dehydrate coseismically and thus also buffer the fault plane temperature. In the case of gypsum dehydration, we have observed that 83% of the enthalpy change is due to the vaporization of water. Above 23 MPa and 647 K, water is supercritical, thus the transition from structurally bonded to supercritical water occurs in a single step, leading to overall elevated enthalpy changes ranging from 100 to 1000 kJ mol<sup>-1</sup> for most dehydration reactions (Robie et al., 1979). At the geological scale, for a given dehydration reaction there is a depth at which the ambient temperature is close to, but below, the equilibrium temperature of the reaction. Assuming an Arrhenius model, a slight temperature increase above this equilibrium temperature induces a dramatic increase of the reaction kinetic, thus allowing a similar process of temperature buffering.

Our microstructural observations (Fig. 4) suggest that geological evidence of coseismic mineral reactions may remain after an earthquake. Field evidence in the gouge of the Chelungpu fault seems to confirm this hypothesis, at least on clay minerals (Hirono et al., 2008). It remains unclear whether such evidence can be preserved over the geological time scale, because rehydration processes may occur. However, the recrystallization and crystal growth features might be a more stable print, if the temperature is high enough for these phenomena to occur.

Understanding the behavior of faults needs complete characterizations, from physical properties of rocks to mineralogical and geological investigations. Because of this complexity, strongly depending on details in the fault rock properties and composition, the possibility of a standard fault zone model could be seriously questioned. Nevertheless, our experiments open the possible existence of a coseismic metamorphism, which, in particular, might explain the low heat flow around active faults and the relative scarcity of pseudotachylytes in nature.

#### ACKNOWLEDGMENTS

We thank T. Togo and K. Oohashi for their help using the apparatus and Hayami Ishisako for thin section preparation. Diane Moore and two anonymous reviewers helped to improve the manuscript. N. Brantut thanks F. Brunet for helpful suggestions and comments. This work was partially funded by INSU (Institut National des Sciences de l'Univers) project 3F.

#### REFERENCES CITED

- Andrews, D.J., 2002, A fault constitutive relation accounting for thermal pressurization of pore fluid: *Journal of Geophysical Research*, v. 107, 2363, doi: 10.1029/2002JB001942.
- Brantut, N., Schubnel, A., Rouzaud, J.-N., Brunet, F., and Shimamoto, T., 2008, High-velocity frictional properties of a clay-bearing fault gouge and implications for earthquake mechanics: *Journal of Geophysical Research*, v. 113, B10401, doi: 10.1029/2007JB005551.
- Brantut, N., Schubnel, A., Corvisier, J., and Sarout, J., 2010, Thermo-chemical pressurization of faults during coseismic slip: *Journal of Geophysical Research*, v. 115, B05313, doi: 10.1029/2009JB006533.
- Di Toro, G., Goldsby, D., and Tullis, T.E., 2004, Friction falls towards zero in quartz rock as slip velocity approaches seismic rates: *Nature*, v. 427, p. 436–439, doi: 10.1038/nature02249.
- Goldsby, D.L., and Tullis, T.E., 2002, Low frictional strength of quartz rocks at subseismic slip rates: *Geophysical Research Letters*, v. 29, 1844, doi: 10.1029/2002GL015240.
- Han, R., Shimamoto, T., Hirose, T., Ree, J.-H., and Ando, J., 2007, Ultralow friction of carbonate faults caused by thermal decomposition: *Science*, v. 316, p. 878–881, doi: 10.1126/science.1139763.
- Han, R., Hirose, T., and Shimamoto, T., 2010, Strong velocity weakening and powder lubrication of simulated carbonate faults at seismic slip rates: *Journal of Geophysical Research*, v. 115, B03412, doi: 10.1029/2008JB006136.
- Hirono, T., Fujimoto, K., Yokoyama, T., Hamada, Y., Tanikawa, W., Tadaï, O., Mishima, T., Tanimizu, M., Lin, W., Soh, W., and Song, S.-R., 2008, Clay mineral reactions caused by frictional heating during an earthquake: An example from the Taiwan Chelungpu fault: *Geophysical Research Letters*, v. 35, L16303, doi: 10.1029/2008GL034476.
- Hirose, T., and Bystricky, M., 2007, Extreme dynamic weakening of faults during dehydration by coseismic shear heating: *Geophysical Research Letters*, v. 34, L14311, doi: 10.1029/2007GL030049.
- Hirose, T., and Shimamoto, T., 2005, Growth of molten zone as a mechanism of slip weakening of simulated faults in gabbro during frictional melting: *Journal of Geophysical Research*, v. 110, B05202, doi: 10.1029/2004JB003207.
- Lachenbruch, A.H., 1980, Frictional heating, fluid pressure, and the resistance to fault motion: *Journal of Geophysical Research*, v. 85, p. 6097–6112, doi: 10.1029/JB085iB11p06097.
- Lachenbruch, A.H., and Sass, J.H., 1980, Heat flow and energetic of the San Andreas fault zone: *Journal of Geophysical Research*, v. 85, p. 6185–6222, doi: 10.1029/JB085iB11p06185.
- Mase, C.W., and Smith, L., 1985, Pore-fluid pressures and frictional heating on a fault surface: *Pure and Applied Geophysics*, v. 122, p. 583–607, doi: 10.1007/BF00874618.
- Mase, C.W., and Smith, L., 1987, Effects of frictional heating on the thermal, hydrologic, and mechanical response of a fault: *Journal of Geophysical Research*, v. 92, no. B7, p. 6249–6272, doi: 10.1029/JB092iB07p06249.
- Rice, J.R., 1999, Flash heating at asperity contacts and rate-depend friction: *Eos (Transactions, American Geophysical Union)*, v. 80, fall meeting supplement, abs. S21D–05.
- Rice, J.R., 2006, Heating and weakening of faults during earthquake slip: *Journal of Geophysical Research*, v. 111, B05311, doi: 10.1029/2005JB004006.
- Robie, R.A., Hemingway, B.S., and Fisher, J.R., 1979, Thermodynamic properties of minerals and related substances at 298.15 K and 1 bar (10<sup>5</sup> pascals) pressure and at higher temperatures: *U.S. Geological Survey Bulletin*, 1452, 456 p.
- Shimamoto, T., and Hirose, T., 2006, Reproducing low- to high-velocity fault motion in fluid-rich environments: An experimental challenge and preliminary results: *Geophysical Research Abstracts*, v. 8, EGU06-A-09077.
- Sibson, R.H., 1973, Interaction between temperature and pore-fluid pressure during earthquake faulting—A mechanism for partial or total stress relief: *Nature*, v. 243, p. 66–68.
- Sibson, R.H., 2003, Thickness of the seismic slip zone: *Seismological Society of America Bulletin*, v. 93, p. 1169–1178, doi: 10.1785/0120020061.
- Sibson, R.H., and Toy, V.G., 2006, The habitat of fault-generated pseudotachylyte: Presence vs. absence of friction-melt, *in* Abercrombie R., et al., eds., *Earthquakes: Radiated energy and the physics of faulting*: American Geophysical Union Geophysical Monograph 170, p. 153–166.
- Solum, J.G., Hickman, S.H., Lockner, D.A., Moore, D.E., Van der Pluijm, B.A., Schleicher, A.M., and Evans, J.P., 2006, Mineralogical characterization of protolith and fault rocks from the SAFOD Main Hole: *Geophysical Research Letters*, v. 33, L21314, doi: 10.1029/2006GL027285.
- Sulem, J., and Famin, V., 2009, Thermal decomposition of carbonates in fault zones: Slip-weakening and temperature-limiting effects: *Journal of Geophysical Research*, v. 114, B03309, doi: 10.1029/2008JB006004.
- Sulem, J., Vardoulakis, I., Ouffroukh, H., Boulon, M., and Hans, J., 2004, Experimental characterization of the thermo-poro-mechanical properties of the Aegion fault gouge: *Comptes Rendus Geoscience*, v. 336, p. 455–466.
- Togo, T., Shimamoto, T., Ma, S., and Hirose, T., 2009, High-velocity friction of faults: A review and implication for landslide studies, *in* *Proceedings: The Next Generation of Research on Earthquake-Induced Landslides: An International Conference in Commemoration of 10th Anniversary of the Chi-Chi Earthquake*: Jungli, Taiwan, National Central University, p. 205–216.

Manuscript received 27 May 2010  
 Revised manuscript received 4 August 2010  
 Manuscript accepted 10 August 2010

Printed in USA